BBA - Biomembranes 1862 (2020) 183349

Contents lists available at ScienceDirect

BBA - Biomembranes

journal homepage: www.elsevier.com/locate/bbamem

The binding of the APT1 domains to phosphoinositides is regulated by metal ions *in vitro*

Damian Kolakowski, Joanna Kaminska*, Teresa Zoladek

Institute of Biochemistry and Biophysics Polish Academy of Sciences, Pawinskiego 5A, 02-106 Warsaw, Poland

ARTICLE INFO

Keywords:
Chorein
Vps13
Atg2
Yeast model
APT1 domain
Protein-lipid interaction
Calcium

ABSTRACT

Chorein is a protein of the Vps13 family, and defects in this protein cause the rare neurodegenerative disorder chorea-acanthocytosis (ChAc). Chorein is involved in the actin cytoskeleton organization, calcium ion flux, neuronal cell excitability, exocytosis and autophagy. The function of this protein is poorly understood, and obtaining this knowledge is a key to finding a cure for ChAc. Chorein, as well as the Vps13 protein from yeast, contains the APT1 domain. Our previous research has shown that the APT1 domain from yeast Vps13 (yAPT1v) binds phosphatidylinositol 3-phosphate (PI3P) *in vitro*. In this study, we showed that although the APT1 domain from chorein (hAPT1) binds to PI3P it could not functionally replace yAPT1v. The hAPT1 domain binds, in addition to PI3P, to phosphatidylinositol 5-phosphate (PI5P). The binding of hAPT1 to PI3P, unlike the binding of yAPT1v to PI3P, is regulated by the bivalent ions, calcium and magnesium. Regulation of PI3P binding via calcium is also observed for the APT1 domain of yeast autophagy protein Atg2. The substitution I2771R, found in chorein of patient suffering from ChAc, reduces the binding of the hAPT1 domain to PI3P and PI5P. These results suggest that the ability of APT1 domains to bind phosphoinositides is regulated differently in yeast and human protein and that this regulation is important for chorein function.

1. Introduction

Vps13 proteins are preserved in all eukaryotic organisms. There is one member of the Vps13 protein family in yeast and four in humans. Human Vps13 proteins, encoded by the *hVPS13A* (9q21.2), *B* (8q22.2), *C* (15q22.2) and *D* (1p36.22) genes, are associated with several neurological disorders. The *hVPS13A* gene encodes chorein, defects in which cause chorea-acanthocytosis (ChAc) [1–4], an ultra-rare hereditary neurological disorder that manifests in patients as difficulties in movement, presence of acanthocytes (spiked red blood cells) and progressive neurodegeneration [5,6]. Little is known regarding the molecular mechanism of ChAc pathogenesis. Various studies have shown several changes in cell physiology, such as alterations in actin cytoskeleton network formation [7,8] calcium (Ca^{2+}) ion flux [9], neuronal cell excitability [10], exocytosis [11] and autophagy [12]. Some of these defects appear to be due to changes in cellular signalling via the tyrosine kinase Lyn and phosphoinositide 3-kinase (PI3K) [13,14]. More is known about the Vps13 protein from yeast (hereafter referred to as Vps13), which shares approximately 40% similarity with chorein [2]. Thus, the studies conducted on the Vps13 protein could be considered as a source of information regarding the possible functions of chorein.

Different Vps13 proteins have been shown to localize to various membrane contact sites (MCSs), where membranes of two different organelles are in close proximity [15,16]. The MCS structure is regulated in response to growth conditions and changes in cell metabolism [17], and MCSs are involved in lipid and ion transport, lipid biosynthesis, and communication between organelles. On glucose-containing media, Vps13 was detected in vacuole and mitochondria patches (vCLAMPs) [18] or endosome-mitochondria MCSs [19], but on glycerol-containing media, Vps13 was detected in nuclear vacuole junctions (NVJs) [20]. In addition, amino acid substitutions in Vps13 allow this protein to compensate for the lack of the Mmm1 protein, a subunit of the endoplasmic reticulum (ER)-mitochondria encounter structure (ERMES), which is the protein complex implicated in ER-mitochondria MCSs formation [18]. Recent data have also shown the

Abbreviations: aa, amino acid residues; ChAc, chorea-acanthocytosis; CPY, carboxypeptidase Y; NVJ, nuclear vacuole junction; PI, phosphatidylinositol; PIPs, phosphoinositides phosphatidylinositol phosphates; PI3P, phosphatidylinositol 3-phosphate; PI5P, phosphatidylinositol 5-phosphate; PI4P, phosphatidylinositol 4-phosphate; PI(4,5)P_2, phosphatidylinositol 4,5-bisphosphate; PA, phosphatidic acid; LPA, lysophosphatidic acid; PH, pleckstrin homology; vCLAMP, vacuole and mitochondria patch

* Corresponding author.
E-mail address: kaminska@ibb.waw.pl (J. Kaminska).

https://doi.org/10.1016/j.bbamem.2020.183349
Received 17 January 2020; Received in revised form 27 April 2020; Accepted 7 May 2020
Available online 11 May 2020

presence of chorein in ER-mitochondria or ER-lipid droplet MCSs and hVps13C in ER-endosome or ER-lipid droplet MCSs [21,22]. Moreover, the ability of the N-terminal part of Vps13 to transfer glycerolipids between liposomes was demonstrated in an *in vitro* assay [21]. The pivotal function of Vps13 proteins is perhaps lipid transfer in MCSs. However, the mechanism by which Vps13 localizes to different MCSs remains to be determined.

The Vps13 of *Saccharomyces cerevisiae* is a large 358-kDa protein with several domains, including the Vps13 Adaptor Binding (VAB) domain (WD-40 like) [23], the APT1 [24] and PH-like domains in the C-terminal part [23,25]. This domain structure is conserved and the WD-40 like, APT1 and PH-like domains are also present in chorein [21,25]. All of the listed domains could participate in establishing different MCSs. This could be achieved by interaction with phosphoinositides (PIPs), a class of short-lived membrane phospholipids that mediate crucial cellular functions via recruitment of proteins containing specific domains. Indeed, many of the domains/regions of Vps13 were documented to be able to bind lipids *in vitro*. The N-terminal part (amino acids residues (aa) 1–437) interacts with phosphatidic acid (PA) and phosphoinositides (PIPs), such as phosphatidylinositol 4-phosphate (PI4P) and phosphatidylinositol 4,5-bisphosphate PI(4,5)P_2, while the C-terminal part (aa 2905–3144) binds to PI(4,5)P_2. The central region (aa 2158–2575) binds all PIPs, PA and lysophosphatidic acid (LPA) [26]. We described the APT1 (yAPT1v) domain (aa 2492–2844) as interacting almost exclusively with phosphatidylinositol 3-phosphate (PI3P) [24]. Recent investigations show that targeting of Vps13 to different membranes is mediated not only by lipid binding, but also by interaction with several adaptor proteins via PxP motifs present in the VAB domain [27]. Modulation of the interaction of Vps13 proteins with different partners (lipids and proteins) is important because this modulation influences Vps13 localization and thus abolishes or promotes its function at particular locations.

Ca^{2+} ions play a significant role in cellular signalling [28]. Several proteins are molecular sensors that are sensitive to Ca^{2+} ions. Many of these proteins are lipid-binding proteins that bind to membranes and are regulated by the presence of Ca^{2+}. Some examples of these proteins are synaptotagmin-1, which binds Ca^{2+} cooperatively with PI(4,5)P_2 [29], and protein kinase C, which interacts with the lipid bilayer in the presence of Ca^{2+} [30]. Upon binding to Ca^{2+}, proteins are able to change their conformation and charge, which ultimately affects their potential interactions and signal transduction. Magnesium (Mg^{2+}) ions are essential without any known specific regulatory functions. The concentration of these ions in the cell is relatively high. There are few reports describing the role of Mg^{2+} in the regulation of the ability of proteins to bind phospholipids. Some reports state that the synaptotagmin-3 protein acts as a Mg^{2+}-dependent sensor of negatively charged phospholipids [31,32].

The Atg2 protein, which belongs to the family of autophagy-related proteins, shares sequence similarity at the N- and C-terminal region to chorein. We documented that the Atg2 possesses the APT1 domain (yAPT1a) domain which binds PI3P [33]. Recently, it was shown that the N-terminal fragment of Atg2, similar to N-terminal part of Vps13, transfers lipids *in vitro* [34].

Previously, we reported that the yAPT1a and yAPT1v domains bind PI3P [24,33]. Here, we studied the lipid binding specificity of the APT1 domain from chorein (hAPT1) in comparison to those of the yeast Vps13 and Atg2 proteins and the effect of Ca^{2+} and Mg^{2+} ions on the binding of APT1 domains to PIPs. We found that the hAPT1 domain, similar to yAPT1a and yAPT1v, binds PI3P and that this binding is regulated by bivalent cations. Moreover, we show that the hAPT1 domain is able to bind PI5P and this binding is not regulated by metal ions.

2. Materials and methods

2.1. Strains, media and growth conditions

The *E. coli* strain XL1-Blue (Stratagene, San Diego, USA) was used for plasmid propagation. The *E. coli* strain SoluBL21 (Genlantis, San Diego, USA) was used for heterologous expression of proteins. The yeast *S. cerevisiae* strains used in this study include BY *MET15* (*MAT**a** his3Δ1 leu2Δ0 MET15 ura3Δ0)* and BY *MET15 vps13Δ (MAT**a** his3Δ1 leu2Δ0, MET15 ura3Δ0 vps13Δ::KanMX)* (W. Rzepnikowska, PhD thesis).

E. coli cells were grown in liquid LB medium supplemented with ampicillin at 37 °C for plasmid propagation or at 28 °C for heterologous protein expression. Yeast cells were grown at 28 °C in liquid YPD medium (1% yeast extract, 2% bactopeptone, 2% glucose) or in synthetic complete medium (SM; 0.67% yeast nitrogen base without amino acids, 2% glucose) with the appropriate supplements (uracil and amino acids) if plasmid selection was required. For the growth test, the cells were grown overnight in SC-ura medium, pelleted and resuspended to OD_{600} = 1 in water, and 1:4 serial dilutions were prepared. Aliquots of each dilution were spotted on YPD plates (YPD, 2.5% agar), YPD plates supplemented with 0.0175% sodium dodecyl sulfate (SDS), SC-ura minimal plates (SC, 2.5% agar) with required supplements and SC-ura-arg plates supplemented or not with 2 μg ml^{-1} L-canavanine and then incubated at 28 °C for 3–5 days.

2.2. Plasmids and plasmid construction

The plasmids used in this study are listed in Table S1. Plasmids with chimeric *VPS13* genes were constructed by homologous recombination in *E. coli* [35]. First, 2388-bp *Sal*I/*Sal*I fragment from pUG35-VPS13 was cloned into pBluescript2SK+, and fragment missing approximately 1100-bp corresponding to yAPT1v was amplified by PCR. Two products, namely, 1124-bp *hVPS13A-hAPT1* and 1124-bp *hVPS13A-hAPT1-I2771R*, flanked by sequences homologous to appropriate sites in *vps13* fragments cloned previously into pBluescript2SK+, were produced. The 4249-bp or 3826-bp PCR products were mixed with the 1124-bp *hVPS13A-hAPT1* or 1124-bp *hVPS13A-hAPT1-I2771R* PCR products, and these mixtures were transformed into *E. coli.* After isolation, the proper plasmids were digested with *Sal*I and cloned into pUG35-VPS13 *Sal*I/*Sal*I to yield pDK305 or pDK306.

The pDK304 plasmid was constructed by one-step site-directed mutagenesis. pBluescript2SK+ plasmids with a 2388-bp *Sal*I/*Sal*I fragment from digested pUG35-VPS13 were amplified by PCR. The PCR product lacking an approximately 1100-bp fragment coding for yAPT1v was self-ligated. After isolation, the plasmid was digested with *Sal*I and cloned into pUG35-VPS13 *Sal*I/*Sal*I.

For the production of truncated chorein variants in *E. coli*, appropriate constructs encoding N-terminally GST-tagged proteins were created. The pKF463 vector, encoding the GST tag alone, was used as a control. This vector is based on the pGEX-4T-1 backbone and carries a STOP codon directly downstream of the encoded TEV protease cleavage site [33]. Appropriate *hVPS13A* fragments were PCR-amplified from p415-P_{TEF1}-hVPS13A and cloned into pKF463. The *hVPS13A-hAPT1* or *hVPS13A-hAPT1* fragments encoding the hAPT1 (aa S2465-P2869) or truncated hAPT1^{s} (aa S2465-V2858) domain were cloned as a 1260-bp *Bam*HI/*Sal*I or 1227-bp *Bam*HI/*Sal*I fragment into the 4960-bp *Bam*HI/*Sal*I-digested pKF463 to obtain pDK101 or pDK101C. The I2771R mutation was introduced into the *hVPS13A-hAPT1* sequence by one-step site-directed mutagenesis of pDK101. Then, the 1260-bp *Bam*HI/*Sal*I fragment was cloned into the 4960-bp *Bam*HI/*Sal*I-digested pKF463 to obtain pDK125.

2.3. Western blot analysis

Yeast cells were grown at 28 °C on SC-ura to the logarithmic phase. Protein extracts were prepared after disrupting cells with glass beads in 2× electrophoresis sample buffer (120 mM Tris-HCl (pH 6.8), 2% SDS, 20% glycerol, 0.04% bromophenol blue, 10% β-mercaptoethanol). Samples were analysed by standard SDS-PAGE followed by Western blot analysis using mouse monoclonal anti-GFP (Roche, Basel, Switzerland), anti-NEDD4 (Millipore, Darmstadt, Germany), and secondary anti-mouse IgG horseradish peroxidase (HRP)-conjugated antibodies (Dako, Glostrup, Denmark), and the signal was developed by using enhanced chemiluminescence substrate (Millipore, Burlington, USA) and detected with a CCD camera (AlphaInnotech, Genetic Technologies, Miami, USA).

2.4. Purification of the Vps13 protein fragments

Truncated variants of chorein, Vps13 or Atg2 were expressed as N-terminally GST-tagged recombinant proteins in the *E. coli* SoluBL21(DE3) strain propagated at 28 °C in LB medium supplemented with 0.2% glucose and 100 μg ml^{-1} ampicillin (Sigma-Aldrich, Saint Louis, USA) for plasmid maintenance. Expression was induced with 0.1 mM IPTG for 1 h. Then, the cells were pelleted, resuspended in equilibration buffer (125 mM Tris-HCl (pH 7.5), 150 mM NaCl) supplemented with protease inhibitor cocktail (Complete Mini, EDTA free, Roche) and lysed by sonication. The homogenate was centrifuged at 20000 ×*g* for 15 min at 4 °C. The supernatant was supplemented with 1 mM DL-dithiothreitol (DTT) and incubated with glutathione magnetic beads (Thermo Scientific, Waltham, USA) for 2 h at 4 °C. After washing, the bound proteins were eluted with 25 mM reduced glutathione in elution buffer (125 mM Tris·HCl (pH 8.0), 150 mM NaCl, 1 mM DTT), and the integrity of the eluted proteins was analysed by Western blotting.

2.5. Protein lipid overlay assay

The identification of lipids interacting with a given protein was performed by an overlay assay. A membrane containing lipids (PIP strips; Echelon Biosciences Inc., Salt Lake City, UT, USA) was blocked with 3% fatty-acid-free BSA (Sigma-Aldrich) in TBS-T (TBS + 0.1% Tween-20) for 1 h at room temperature and then incubated overnight at 4 °C in blocking buffer with 0.5–1 μg ml^{-1} of a particular protein or GST alone as a negative control. Bound proteins were detected by Western blot with anti-GST HRP-conjugated antibodies (BioLegend, San Diego, USA).

2.6. Liposome binding assay

Liposomal assays were carried out using synthetic biotin-tagged PolyPIPosomes containing 5% (w/w) individual PIPs, 65% (w/w) phosphatidylcholine, 29% (w/w) phosphatidylethanolamine, and 1% (w/w) biotin (Echelon Biosciences Inc.). The purified proteins GST-hVps13A-(hAPT1), GST-hVps13A-I2749R-(hAPT1*), GST-Vps13-(yAPT1v), GST-Atg2-(yAPT1a), and GST-hVps13A-($hAPT1^s$) or GST alone as a negative control were incubated with 5 μl of the liposome mixtures in 0.8 ml of reaction buffer (50 mM HEPES (pH 7.5), 150 mM NaCl) supplemented with 2 mM EDTA, 1 mM Mg^{2+} or 1 mM Ca^{2+} for 30 min at room temperature. Next, 50 μl of Dynabeads MyOne Streptavidin C1 (Invitrogen) was added to pull down the lipid-protein mixtures and incubated for 1 h at 4 °C. Following 5 washes with 0.5 ml of reaction buffer, the beads were mixed with 2× sample buffer (120 mM Tris-HCl (pH 6.8), 2% SDS, 20% glycerol, 0.04% bromophenol blue, 10% β-mercaptoethanol, 8 M urea) and processed for Western blot analysis using anti-GST HRP-conjugated antibodies (BioLegend). After the reaction, the supernatants were collected and concentrated in Amicon centrifugal filters (Merck). The buffer in these samples was exchanged with 8 M urea, and 4× sample buffer was added. Densitometry analysis of the blots was performed with ImageJ (https://imagej.nih.gov/ij/). Chart and statistical analyses were performed in GraphPad Prism.

2.7. Ca^{2+}-binding site prediction

To model the potential Ca^{2+} ion-binding sites of the APT1 domains, the IonCom server (https://zhanglab.ccmb.med.umich.edu/IonCom/) was used. The amino acid residue sequences used for the prediction correspond to the fragments of the chorein (hAPT1), yeast Vps13 (yAPT1v) and Atg2 (yAPT1a) proteins used in the protein-lipid overlay assay and in the liposome binding assay. The sequences were hAPT1, aa 2515–2919 (UniProt), yAPT1v, aa 2492–2844 and yAPT1a, aa 1079–1417 (*Saccharomyces* Genome Database).

2.8. Bioinformatics analysis

Protein homology detection and structure prediction was performed through HHpred [36] and Phyre2 [37].

3. Results

3.1. The APT1 domain of chorein differs from that of Vps13

We previously found that the phenotypes caused by the *VPS13* gene deletion (*vps13Δ*) in yeast are not complemented by the cDNA of *hVPS13A* [24]. Thus, to learn more about the function of chorein and its domains, we focused on the APT1 domain. Earlier studies showed that the APT1 domain, which we identified in the Vps13 and Atg2 proteins, binds PI3P and that it is essential for proper functioning of the Vps13 protein [24,33]. A region with homology to the APT1 domain was also found in chorein (aa 2600–2854) (probability: 97.03%, E value 0.00016, score 96.5) as determined by hidden Marcov model (HMM) mapping using HHPred (Fig. S1) (http://toolkit.lmb.uni-muenchen.de/hhpred). It is worth noting that all of the APT1 domains that we characterized lacked N-terminus in contrast to the APT1 domain described in the Pfam database. Because the hAPT1 domain that we identified potentially overlaps with the DH-like domain (aa 2751–3027) determined by Kumar et al. (Fig. S2) [21], we additionally performed bioinformatic analysis of chorein using Phyre2. Our analysis indicated that the DH-like fold (fold id: c4uosA) starts at aa 2871 and thus is located after the APT1 domain (Fig. S2).

Here, we documented whether the APT1 domain of Vps13 is interchangeable with that of chorein. A domain swap experiment was performed. We constructed yeast expression plasmid encoding chimeric protein consisting of a Vps13 protein in which the yAPT1v domain (aa 2498–2844) was swapped with a domain originating from chorein, hAPT1 (aa 2504–2869) (Fig. 1A). The fragments we exchanged had additional N- and C-terminal unstructured flanks, as predicted by Phyre2. In addition, the yAPT1v domain was also substituted for the mutant hAPT1*, with an amino acid residue substitution found in ChAc patient-derived chorein (I2771R). All chimeric proteins were GFP tagged on the C-terminus because *VPS13-GFP* complemented all the phenotypes of *vps13Δ* that we analysed, and *VPS13-GFP* was used as a control. Next, the levels of the chimeric proteins in the yeast *vps13Δ* strain transformed with the respective plasmids were tested. Western blot analysis with anti-GFP antibodies demonstrated that all the chimeric proteins of appropriate molecular weights were produced (Fig. 1B). This result allowed us to investigate the functionality of chimeric proteins by analysing selected *vps13Δ* mutant phenotypes, such as hypersensitivity to SDS [38] and canavanine [24]. The *vps13Δ* strain was transformed with plasmids encoding all tested chimeric proteins and with control plasmids encoding the wild-type Vps13 protein (Vps13-GFP), Vps13 lacking the yAPT1v domain (Vps13-APT1Δ-GFP) or with an empty vector. Only a transformant bearing full-length

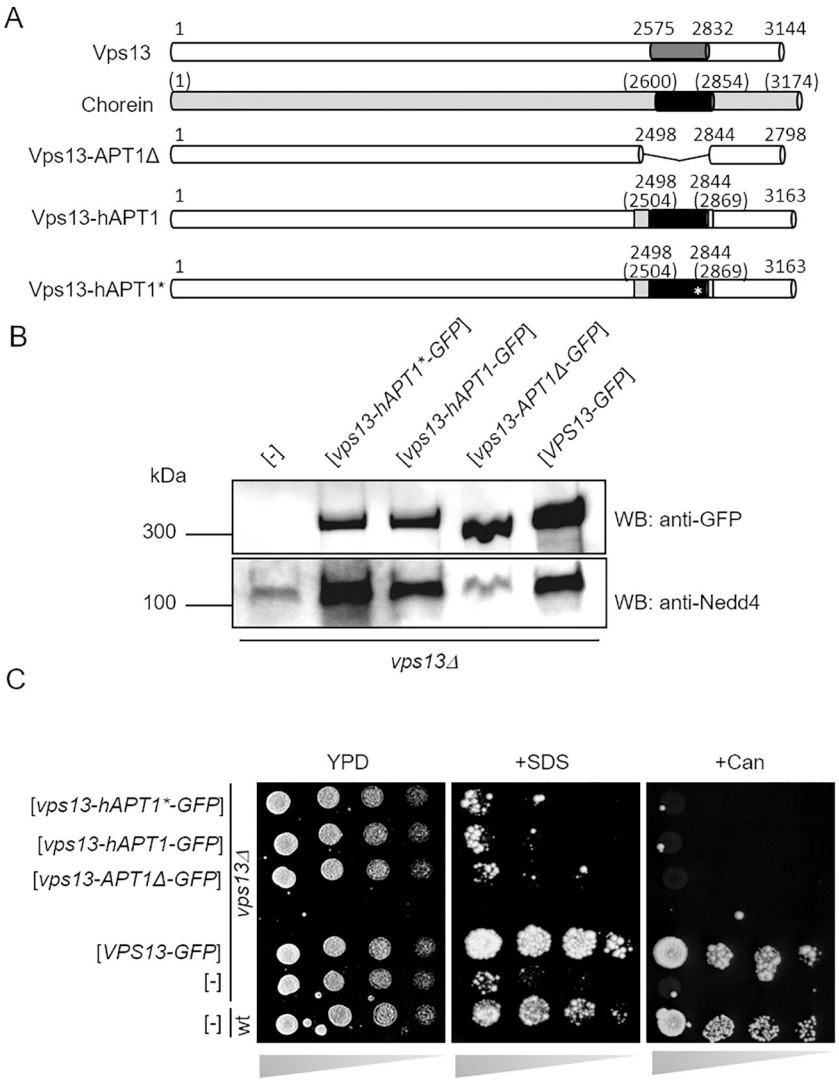

Fig. 1. APT1 domains of Vps13 and chorein are not interchangeable. (A) Schematic representation of the Vps13 protein, its truncated variant, chorein, and chimeric Vps13 consisting of a Vps13 protein in which the yAPT1v domain was swapped with a hAPT1 domain originating from chorein. The APT1 domains are indicated (yAPT1v in dark grey and hAPT1 in black). The numbering of amino acid residues in Vps13 and chorein is given; numbers in brackets correspond to respective amino acid residues in the chorein. The position of the isoleucine (I) residue substituted for arginine (R) in ChAc patients (I2771R) is indicated by asterisk. (**B**) The level of the fusion proteins described in (A) in yeast *vps13Δ*. All proteins were GFP tagged at the C-terminus. Cells were transformed with plasmids bearing indicated alleles or empty vector [−] and grown. Total protein extracts were prepared and analysed by SDS-PAGE followed by Western blotting with anti-GFP and anti-Nedd4 antibodies recognizing Rsp5 (loading control). (**C**) Sensitivity of yeast strains to SDS and L-canavanine. Serial 4-fold dilutions of wild-type and *vps13Δ* strains bearing the indicated plasmids were spotted on YPD and YPD supplemented with 0.0175% SDS or the synthetic medium SC-arg-ura supplemented with 3 μg ml^{-1} L-canavanine (+Can) and incubated at 28 °C for 2–7 days.

yeast *VPS13-GFP* on a plasmid was able to grow on SDS- or canavanine-containing plates, which revealed that under the tested conditions, the yeast-human fusion *VPS13* gene was not able to complement the lack of *VPS13* (Fig. 1C). Thus, the hAPT1 domain was not able to replace the yAPT1v domain, suggesting that APT1 domains from yeast and human Vps13 proteins differ significantly, even though their GFP-fusions were similarly located in cells (Fig. S5), or the hAPT1 domain blocks the action of the rest of the Vps13 protein. To identify the reason for the observed difference between the yAPT1v and hAPT1 domains, we determined whether they have different lipid partners.

We analysed the lipid binding of hAPT1 using a protein-lipid overlay assay. The mutant hAPT1* domain was included into our analysis to determine whether a pathogenic amino acid residue substitution affects lipid binding. The recombinant hAPT1 and hAPT1* fused to GST (Fig. S3A) were tested for different glycerophospholipid binding abilities. The analysis revealed that hAPT1 binds PI3P (Fig. S3B) similar to the yAPT1v domain [24], but also binds phosphatidylinositol 5-phosphate (PI5P) and phosphatidylinositol 4-phosphate (PI4P) (Fig. S3B). There was no difference in phospholipid binding specificity between the hAPT1 and hAPT1* domains in this assay (Fig. S3B). Thus, we found that the difference between the APT1 domains of Vps13 and chorein is the ability to bind PI5P and PI4P; hAPT1 can bind PI5P and PI4P, while yAPT1v cannot. This result confirmed our hypothesis that the hAPT1 and yAPT1v domains may differ in lipid binding specificity and prompted us to investigate this finding further. We concentrated on binding of APT1 domains to PI5P and PI3P. The characterization of their binding to PI4P remains for further studies.

3.2. hAPT1 binds PI3P in a bivalent-cation-dependent manner

To confirm the difference between the APT1 domains that we observed in the protein-lipid overlay assay, the ability of GST-APT1 domain fusions (of both yeast and human origin; Fig. 2A) to bind PI3P- or PI5P-enriched liposomes was tested. Moreover, we also examined how metal ions affect binding. Lipid binding tests were performed in the presence of EDTA chelating ions, in the presence of Mg^{2+} or Ca^{2+} ions. These conditions were tested because the IonCom server (https://zhanglab.ccmb.med.umich.edu/IonCom/) predicted that the hAPT1 domain potentially binds Ca^{2+} ions, while the domain from Vps13 does not (Fig. S4). In all further experiments, biotin-tagged liposomes were used, which were pulled down using streptavidin-covered beads. The amount of recombinant protein bound to the liposomes was monitored by Western blot analysis using an anti-GST antibody. Control experiments were also conducted in which recombinant proteins were incubated with liposomes without PIP enrichment (P0), liposomes with phosphatidylinositol (PI) or without liposomes (-LIP). We previously provided evidence that in a liposome binding assay the yAPT1v domain binds PI3P in Mg^{2+}-containing buffer [24]. Indeed, we recovered approximately 35–45% of the recombinant GST-yAPT1v, which was added to the reaction, on liposomes containing PI3P, and the binding

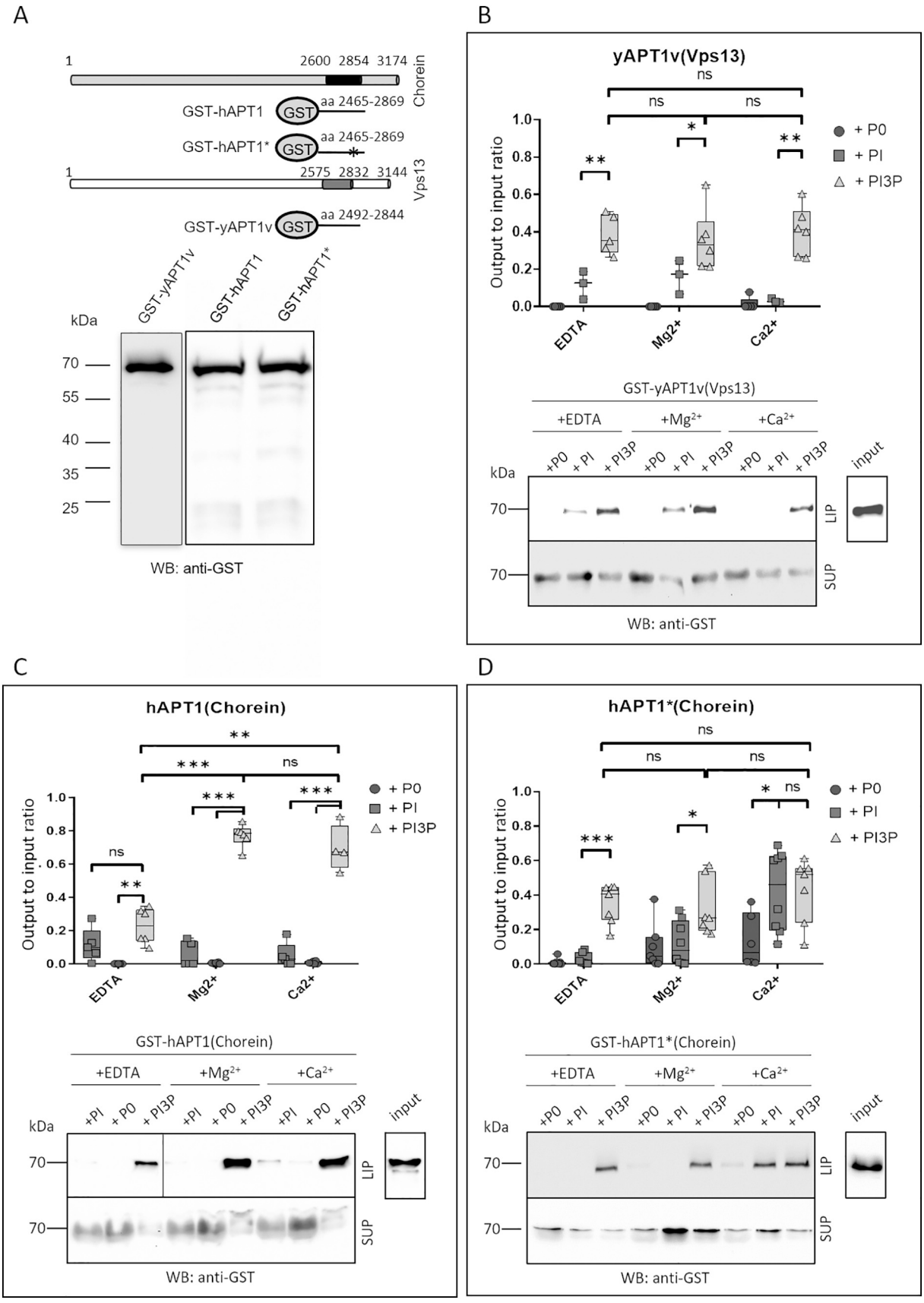

(caption on next page)

Fig. 2. Binding of APT1 domains from Vps13 and chorein to PI- and PI3P-containing liposomes. (**A**) Schematic representation of the Vps13 and chorein with APT1 domains indicated (as in Fig. 1). Fragments fused to GST used in the liposome binding assay are shown. The position of the isoleucine (I) residue substituted for arginine (R) in ChAc patients (I2771) is indicated by an asterisk. Western blot shows purified fragments used for the liposome binding assay. The purified proteins GST-yAPT1v (**B**), GST-hAPT1 (**C**) and GST-hAPT1* (**D**) were incubated with the indicated biotin-tagged liposomes (P0, without any phosphoinositides; PI, liposomes with 5% phosphatidylinositol; PI3P, liposomes with 5% phosphatidylinositol 3-phosphate) in three different conditions: with 2 mM EDTA (+EDTA); 1 mM $MgCl_2$ ($+Mg^{2+}$) or 1 mM $CaCl_2$ ($+Ca^{2+}$). Liposomes were pulled down using streptavidin-covered beads. All the fractions recovered, concentrated supernatants and protein input were loaded onto the gel. The fusion proteins were detected using an anti-GST antibody. The upper panel of the blots shows proteins bound to liposomes (LIP), and the lower panel presents an analysis of the fraction not bound to liposomes (SUP). A representative Western blot result of each analysis is presented. The statistical analysis of the densitometry scans of the Western blots, performed using ImageJ software, is presented. The ratio between proteins bound to particular liposomes and input was calculated. Statistical analysis: mean ± SD; *t*-test; $p < .05$*, $p < .01$**, $p < .001$***; ns, non-significant. Number of repetitions: N = 4–7 depending on experiment.

occurred under all three tested conditions (+EDTA, $+Mg^{2+}$ and $+Ca^{2+}$) with similar affinity (Fig. 2B). Binding to control liposomes containing PI was also observed, but this binding was weak and not statistically significant. No binding to liposomes devoid of any PIPs (P0) was observed.

Interestingly, the binding of the GST-hAPT1 domain to PI3P was found to be regulated. Approximately 20% of the recombinant GST-hAPT1 protein was recovered on PI3P-containing liposomes in the absence of Ca^{2+} and Mg^{2+} ions, which was significantly different from the binding of GST-hAPT1 to control liposomes (P0) but not to PI-containing liposomes (Fig. 2C). In contrast to the EDTA condition, in the presence of both tested cations, significant enhancement of binding (approximately 70%–80%) of the recombinant GST-hAPT1 protein to liposomes containing PI3P was observed (Fig. 2C). Thus, in the presence of Ca^{2+} or Mg^{2+} ions, the binding of hAPT1 to PI3P is preferred over the binding to PI.

The amino acid residue substitution I2749R in the yAPT1v domain, equivalent to the substitution I2771R found in a patient with ChAc, causes a reduction in PI3P binding [24]. For this reason, we also tested the effect of this substitution on the ability to bind PI3P in a natural context, i.e., in the hAPT1 domain. The I2771R mutant (GST-hAPT1*; Fig. 2A) was able to bind PI3P similarly under all studied conditions (+EDTA, $+Mg^{2+}$, $+Ca^{2+}$), but this binding was much weaker than that of wild-type hAPT1 (Fig. 2D). In fact, the binding of the mutant hAPT1* domain to liposomes containing PI3P was at a similar level as that of yAPT1v, which means that 40% of GST-hAPT1* was still recovered on liposomes containing PI3P. Similar to the Vps13 mutant with the I2749R amino acid residue substitution [24], stronger binding of GST-hAPT1* than GST-hAPT1 to PI-liposomes was observed (40% versus 10%, respectively), in the presence of Ca^{2+} ions. In fact, binding of hAPT1* to PI3P-containing liposomes was similar to binding to PI-containing liposomes. Therefore, experiments have shown that substitution of I2771R in hAPT1 changes the affinity of this domain for PI3P and PI, and regulation of PI3P binding by metal ions is lost.

3.3. The yAPT1a domain binds PI3P only in the presence of calcium ions

We next sought to determine how the APT1 domain from yeast Atg2 (yAPT1a) is regulated. The GST-yAPT1a fusion protein was purified (Fig. 3A), and its binding characteristics with PI3P-containing liposomes were investigated under all the conditions tested previously (+EDTA, $+Mg^{2+}$, $+Ca^{2+}$). Surprisingly, GST-yAPT1a was able to bind PI3P only in the presence of Ca^{2+} ions (Fig. 3B). Computational analysis did not predict the ability of yAPT1a to bind Ca^{2+} ions (Fig. S4), suggesting that the effect of Ca^{2+} on PI3P binding must differ. Thus, even if the *in silico* study did not predict Ca^{2+} binding, it seems that binding of Atg2 to membranes can be regulated by the effect of Ca^{2+} ions on the yAPT1a domain. In general, these results showed that the ability to bind PI3P is a characteristic feature of APT1 domains, but there is a difference between domains in terms of the conditions needed for this binding.

3.4. The C-terminally truncated hAPT1 domain loses the bivalent cation-dependent ability to bind PI3P

In the hAPT1 domain, the amino acid residues important for Ca^{2+} binding are located at the C-terminus, as predicted by the IonCom server (Fig. S4). To confirm whether these amino acids are actually responsible for regulation of the cation-dependent binding of hAPT1 to PI3P, we expressed a truncated hAPT1 lacking 11 aa at the C-terminus ($hAPT1^{s}$) (Fig. 4A). This truncated protein was used in tests for binding to liposomes containing PI3P under all the previously tested conditions. The binding of $hAPT1^{s}$ to PI3P was very weak in all conditions and the metal ions Ca^{2+} or Mg^{2+} did not enhance this binding (Fig. 4B). This result indicates that the deleted 11-amino-acid sequence from hAPT1 is necessary for bivalent cation-mediated regulation of PI3P binding. Taken together, these data indicate that the hAPT1 may be a new Ca^{2+}- and Mg^{2+}-dependent PIP-binding domain.

3.5. The PI5P binding properties of the APT1 domain of chorein

As protein-lipid overlay assays revealed, the GST-hAPT1 domain binds strongly to PI5P (Fig. S3B), while binding of GST-yAPT1v to PI5P was not detected [24]. We were interested in whether this binding is dependent on the presence of ions, as in the case of PI3P binding. Hence, in the next step, we compared the APT1 domains of Vps13 and chorein in the context of PI5P binding using the same conditions as described above. Binding of yAPT1v to PI5P-containing liposomes was observed only in the presence of calcium and was very weak; < 10% of the GST-yAPT1v added to the reaction, (Fig. 5A), which was not statistically significant. In contrast, the hAPT1 domain was effectively retained on liposomes containing PI5P, and this binding was not dependent on the presence of cations. In this experiment, 30%–60% of the recombinant hAPT1 protein was found on liposomes containing PI5P (Fig. 5B). The I2771R mutation greatly reduced PI5P binding (to approximately 5% of the input level) in all conditions tested (Fig. 5C). Thus, this analysis suggests that the I2771R mutation present in the chorein of ChAc patient changes lipid binding and probably membrane binding, which reduces the function of this protein at particular cellular locations where PI3P and/or PI5P is present. This finding also indicates that the reduction of chorein binding to specific regulatory lipids, such as PIP, is pathogenic.

4. Discussion

Chorein, a human protein implicated in the neurodegenerative disease chorea-acanthocytosis, has a poorly defined physiological function. Chorein was found to be localized on the membranes of many different organelles. This diversity in localization is achieved via the interaction of its domains and motifs with lipids and proteins. These interactions must be regulated, as indicated by the changes in localization of Vps13 depending on the growth conditions [18]. Our work aimed to characterize the APT1 domain present in chorein, and in yeast Vps13 and Atg2 proteins. Here, we have demonstrated that the hAPT1

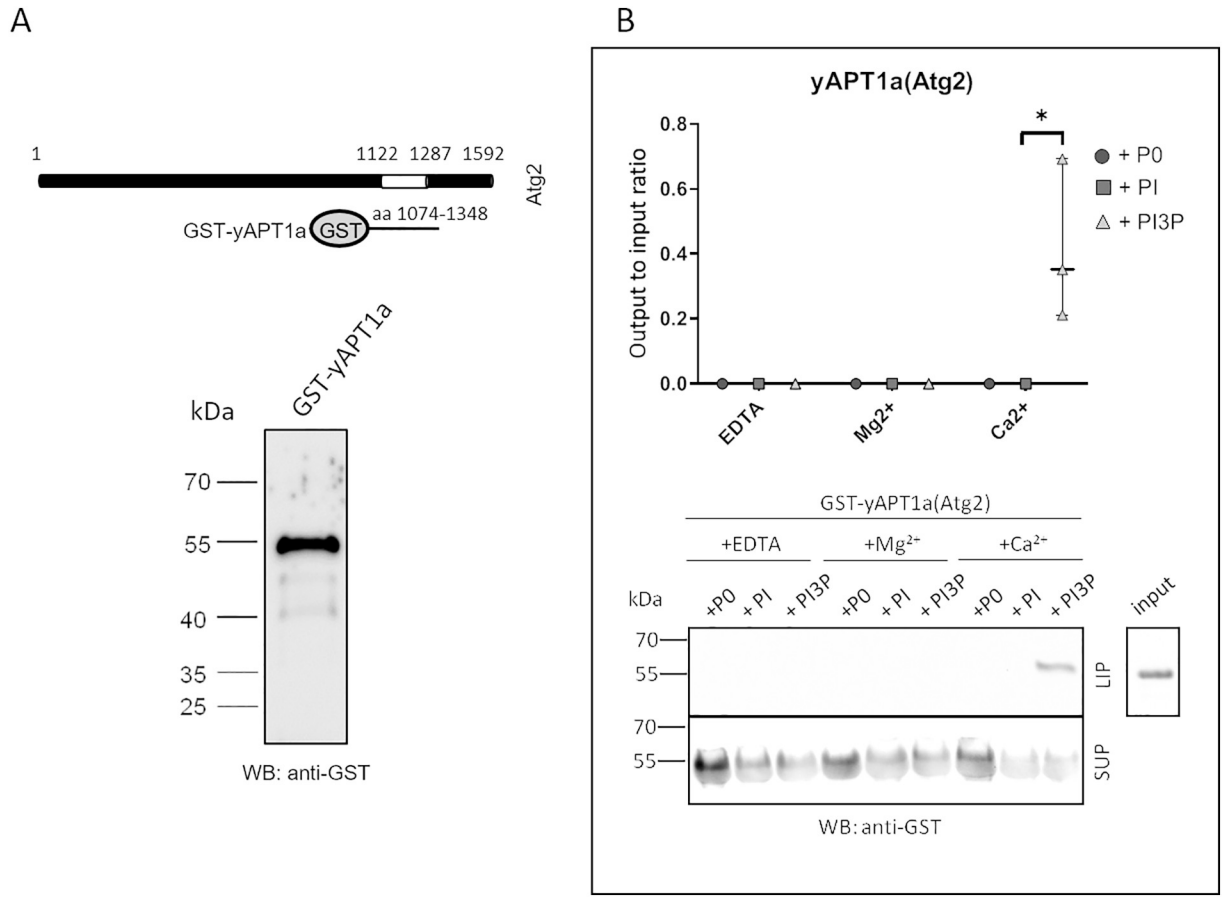

Fig. 3. The influence of calcium on the binding of PI3P by the yAPT1a domain. (**A**) Schematic representation of the Atg2 protein with APT1 domain (yAPT1a in white) and its fragment fused to GST. The Western blot analysis of purified fragment used for the liposome binding assay is shown. (**B**) Interaction of purified GST-yAPT1a protein with PI3P-enriched liposomes was assayed and the statistical analysis was performed as described in Fig. 2. Number of repetitions: N = 3.

domain binds to PI3P, lipid characteristic for endosomal/lysosomal membranes. Our analysis also revealed that APT1 domains of various proteins differ in their ability to bind various PIPs and that hAPT1 interacts not only with PI3P but also with PI5P. Additionally, the ability of different APT1 domains to interact with PIPs is differently regulated by Mg^{2+} and/or Ca^{2+} ions. Both these ions enhanced the binding of the hAPT1 domain to PI3P, and Ca^{2+} ions were necessary for the binding of yAPT1a to PI3P. We showed that the I2771R substitution found in the hAPT1 domain of the ChAc patient changes the interaction with PI3P in a manner similar to the corresponding I2749R substitution in yAPT1v. In addition, we have demonstrated that this substitution abolishes the Ca^{2+} and Mg^{2+} stimulation of PI3P binding and shifts the affinity towards PI. Therefore, our work suggests that chorein might be a protein regulated by calcium signalling, and we propose that the loss of PI3P binding regulation and reduced affinity of mutant hAPT1 for PI5P binding are changes of great importance for cell physiology, they result in ChAc pathogenesis.

Chorein was found to localize to ER-lipid droplet and ER-mitochondria MCSs [21,22]. Nevertheless, chorein may be recruited to many other cellular structures in response to different stimuli or conditions. Although there is no evidence of the localization of chorein on endosomal membranes, Vps13 and hVps13B were found in this compartment [19,39]. In endosomes, PI3P plays a role in the recruitment of effector proteins responsible for the correct sorting of proteins into vacuoles, Golgi apparatus and/or plasma membrane. PI3P is also necessary to regulate fusion of transport vesicles and in the process of autophagy, where it regulates the growth of autophagosome [40]. The Vps13 protein may therefore be one of the PI3P effectors, and its participation in fusion of vesicles [26], protein sorting [41] and autophagy [42] may depend on its recruitment to membranes containing PI3P. Indeed, our previous work has shown that Vps13 not only binds to PI3P, but PI3P also regulates the localization of Vps13 [20,24]. Thus, also binding of chorein to endosomal/lysosomal membranes, enriched with PI3P, might be regulated. Surprisingly, the hAPT1 domain binds not only PI3P but also PI5P and PI4P. The role of PI5P in the cell is poorly understood. It is estimated that PI5P accounts for approximately 0.5% of the PIPs in a cell [43]. In mammalian cells, PI5P is localized to the nucleus and non-nuclear membranes, including the plasma membrane, endosomes ER or Golgi apparatus membranes [44,45]. PI5P plays a crucial role in each of these compartments, where it affects remodelling of the actin cytoskeleton, endocytosis [45–47], and nuclear signalling [48–50]. It was found that the level of PI5P increases under some forms of stress, such as hyperosmotic stress or oxidative stress [43]. Why is the binding of hAPT1 to PI3P regulated by Mg^{2+} and/or Ca^{2+} but the binding to PI5P is not regulated by these ions? This difference can have two explanations: either hAPT1 has a high affinity for PI5P and ions are not required to enhance this interaction or binding to PI5P is otherwise regulated by an interaction with the chorein adapter protein that has not yet been identified. The remaining questions to be answered are regarding the role of PI5P in the regulation of chorein function and localization *in vivo*. There is no evidence for the presence of PI5P in yeast cells. Although Vps13 is important for survival under some forms of stress, such as in the presence of SDS [38] or canavanine [24], it is not clear how this feature can be linked to changes in interactions with lipids. Hence, our results provide information only about the possible role of PI5P as a regulator of chorein. PI5P could recruit chorein to certain locations to facilitate the transfer of lipids to or from membranes containing PI5P. There are also other domains that exhibit PI5P

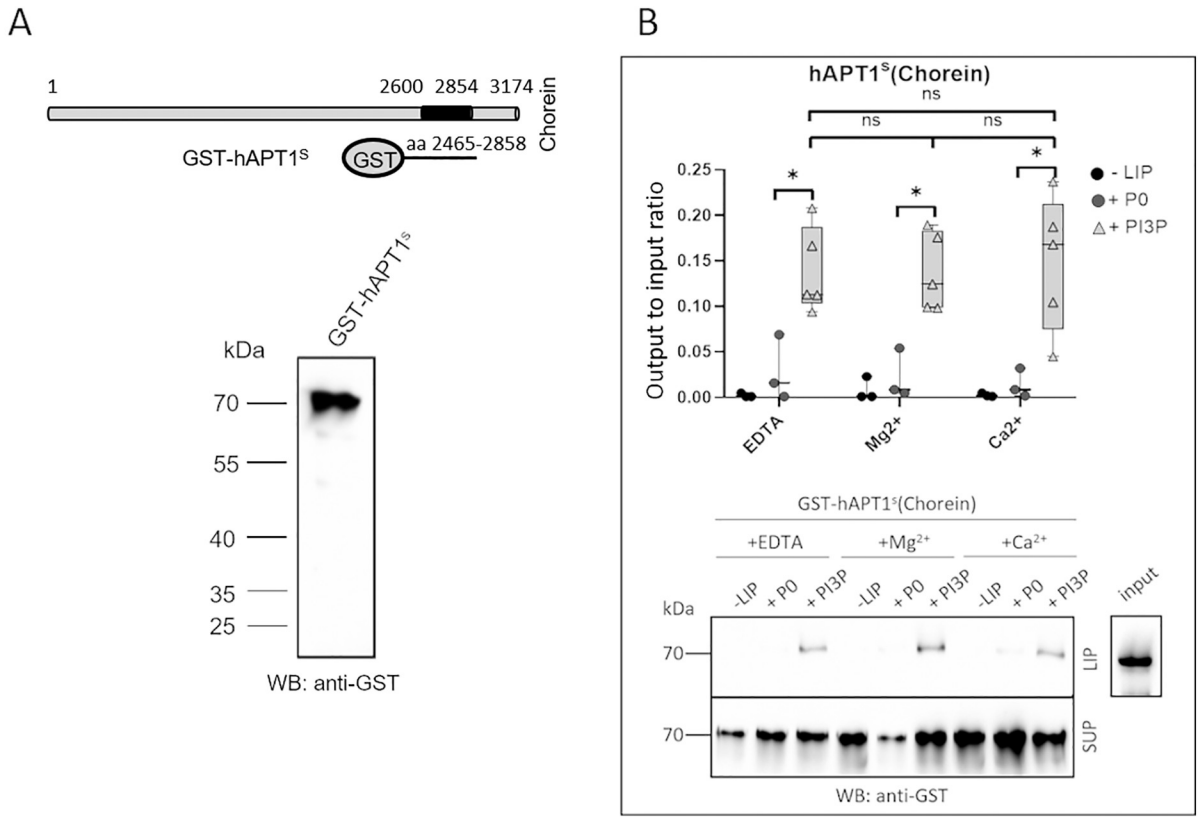

Fig. 4. The influence of calcium on the binding of PI3P by the truncated hAPT1s domain. (**A**) Schematic representation of the chorein (as in Fig. 1) and its shortened APT1 domain (hAPT1^{s}) fused to GST. The Western blot analysis of purified fragment used for the liposome binding assay is shown. (**B**) Interaction of purified GST-hAPT1^{s} protein with PI3P-enriched liposomes was assayed and the statistical analysis was performed as described in Fig. 2. Number of repetitions: N = 5.

binding, such as the VHS domain of the Tom1 protein, known as the PI5P adaptor. It exhibits, in protein lipid overlay assay, a binding profile to different PIPs similar to that of the hAPT1 domain [51]. Additionally, proteins containing the FYVE finger domain, associated mainly with PI3P, may also weakly bind to PI5P [52,53]. Thus, dual lipid binding specificity to PI3P and PI5P has been previously described in the literature and is not a hAPT1-specific feature.

The regulation of the lipid binding activity of the APT1 domain by ions is not surprising, as the interaction of lipids with effector proteins has to be controlled. The C2 domain is an example of a lipid-binding domain, which in some proteins is regulated by Ca^{2+}. Interestingly, C2 domains are also described as having different selectivity for binding to lipids at different Ca^{2+} ion concentrations [54]. The regulation of hAPT1 binding to PI3P by Ca^{2+} may be physiologically significant. Recruitment of yeast Vps13 to endosome and vacuole membranes is most likely achieved by binding the Ypt35 adaptor in response to different conditions [27,55]. However, in yeast binding to Ypt35 may not be sufficient to recruit Vps13 protein to membranes. Binding of the Ypt35 adapter protein and yAPT1v domain to PI3P may act synergistically to increase the recruitment efficiency of Vps13 protein to membranes. Such cooperative membrane binding with several elements is a common feature of many proteins [56]. In the case of hAPT1, the ability of this protein to bind PI3P must be stimulated by the presence of Ca^{2+} or Mg^{2+} ions. Although these ions are available in a cell the hAPT1 cannot replace the yAPT1v domain suggesting that Ca^{2+} ions local concentration may be insufficient. Another possibility is that the chimeric protein, due to its hAPT1 properties, binds PI5P efficiently and is therefore localized on an inappropriate membrane in the yeast cell. However, in yeast cells the PI5P has not been found so far.

Our analysis of fluorescence microscopy images showed that the location of both GFP-yAPT1v and GFP-hAPT1 proteins is similar to that of yAPT1a [33] and coincides with the location of the chaperones of Protein Quality Control (PQC) compartments, Hsp42 and Hsp104 (Fig. S5). Both fusion proteins can be directed to this compartment because are abnormal or Vps13 proteins have their specific role in PQC where are recruited by the regulatory PIPs present in these structures. Recent data show the deposition of misfolded proteins accompanied by Hsp104 near the mitochondria where they co-localize with the Vps13 and Vps39 proteins in MCSs. These MCSs are involved in both physical and functional formation of inclusions and their subsequent removal [57]. This association of aggregates with organelles suggests that specific lipids at these location may provide the necessary environment for disaggregation [57]. In agreement with this idea are results showing that PI3P regulates the yeast cell response to proteotoxic stress [33]. In summary, the analysis indicates that the hAPT1 and yAPT1v domains, similar to the yAPT1a domain of the Atg2 protein, may be responsible for the recruitment of the respective proteins to PQC in response to proteotoxic stress.

The fact that the yAPT1a domain of Atg2 binds PI3P-containing liposomes only in the presence of Ca^{2+} ions indicates that studies of the APT1 domains should be performed in several different conditions, particularly because Ca^{2+} ions binding could not be predicted *in silico*. Our result can explain why Atg2 recruitment to liposomes with PI3P increased only slightly compared to binding to liposomes without PI3P in experiments described by Gómez-Sánchez et al. in which buffers without Ca^{2+} and Mg^{2+} ions were used [58]. This result also suggests that the regulation of the binding of yAPT1a to PI3P by Ca^{2+} must differ from that of hAPT1. It is possible that the yAPT1a domain interacts weakly with PI3P and that Ca^{2+} ions stabilize this binding via one of the mechanisms similar to these described for C2 domain. In case of the C2 domain, Ca^{2+} ions play at least three different roles: (1) Ca^{2+} binding changes the electrostatic potential of the domain; (2) Ca^{2+} ions provide a bridge between the domain and membrane lipids and (3) Ca^{2+} induces conformational changes in the domain/protein, which

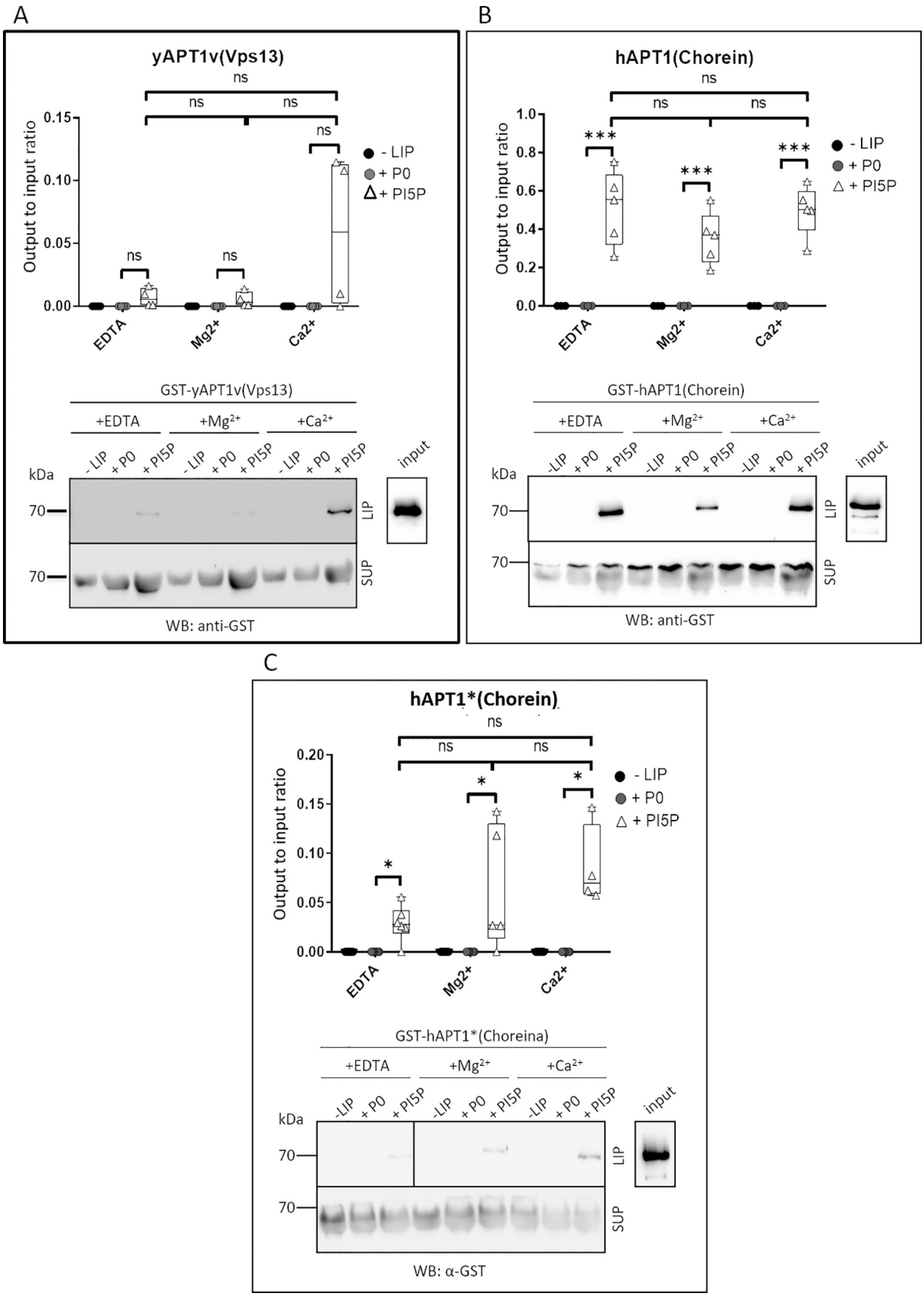

Fig. 5. Binding of the yAPT1v and hAPT1 domains to PI5P-containing liposomes. The purified proteins GST-yAPT1v (**A**), GST-hAPT1 (**B**) and GST-hAPT1* (**C**) were incubated with the indicated liposomes (-LIP no liposomes; P0, lacking any phosphoinositides; PI5P, liposomes with 5% PI5P) in three different conditions, with 2 mM EDTA (+EDTA), 1 mM $MgCl_2$ (Mg^{2+}) or 1 mM $CaCl_2$ (Ca^{2+}). The binding and statistical analyses were performed as in Fig. 2. *t*-test; p < .05*, p < .01**, p < .001***; ns, non-significant. Number of repetitions: N = 4–7. Note that values on the Y axis differ among A, B and C.

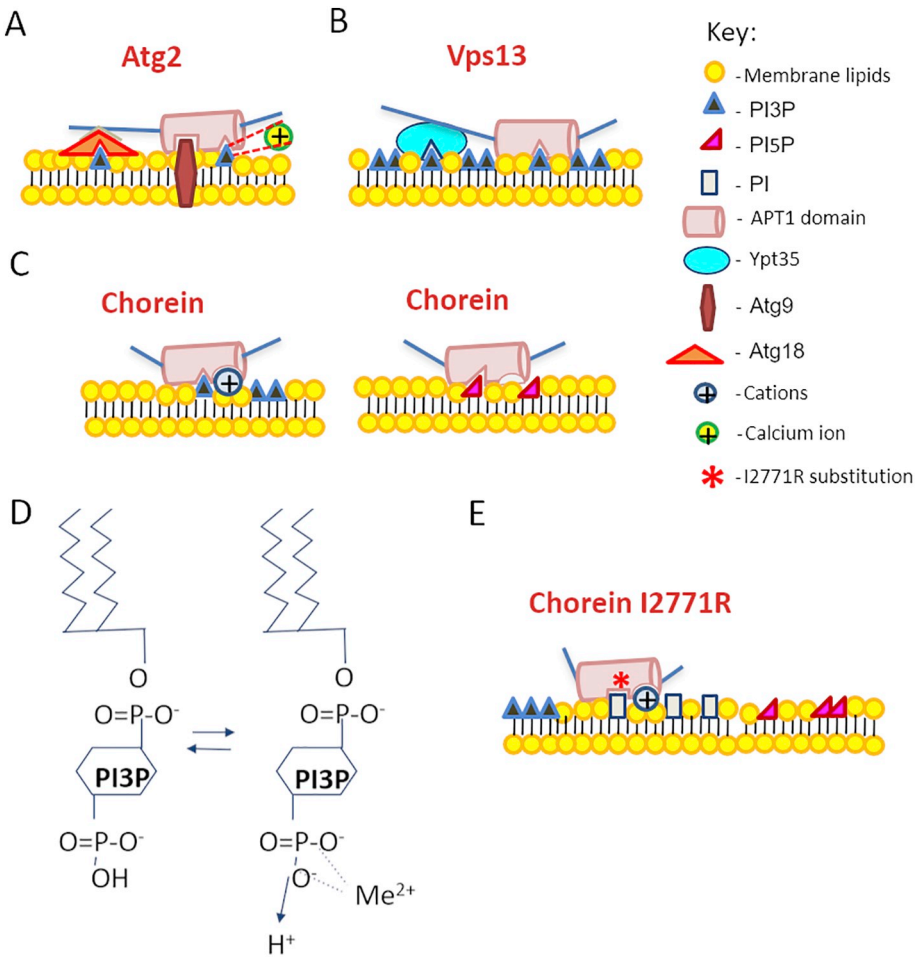

Fig. 6. Model of the regulation of APT1 domains. (**A**) The yAPT1a domain binds to membranes containing PI3P in a calcium-dependent-manner; (**B**) Binding of the yAPT1v domain of Vps13 to membranes containing PI3P and concomitant interaction with the adaptor protein Ypt35; (**C**) The binding of the hAPT1 domain to PI3P regulated by cations; **(D)** Influence of metal ions on the phosphate group of phosphoinositides; **(E)** Lack of regulation by cations due to I2771R substitution in hAPT1 and consequent reduction in the binding to PI3P. See text for details.

triggers interaction [59]. Additionally, the recruitment of Atg2 to membranes within ER-preautophagosome MCS [60] cannot rely only on interaction with lipids, but this process could be stabilized by additional interaction with proteins, such as Atg9 via the APT1 domain [58] and with Atg18 via other domains (Fig. 6A) [61]. The hAtg2A protein interactions seem to be also regulated by Ca^{2+}. In starvation or pharmacologically induced autophagy, the protein of the autophagy machinery WIPI-1, a homologue of yeast Atg18, which is a partner protein of hAtg2A, accumulates in puncta corresponding to phagophore membranes. The occurrence of this puncta is reduced in the presence of BAPTA-AM (1,2-bis(O-aminophenoxy)ethane-N,N,N′,N′-tetra-acetic acid tetra (acetoxymethyl) ester), a Ca^{2+} ion chelator [62]. Importantly, addition of BAPTA-AM does not affect the production of PI3P [62,63], indicating that the localization of the hAtg2A-WIPI-1 complex on the edge of the nascent phagophore depends on the presence of Ca^{2+} ions. This finding can be explained by our result showing that the binding of the yAPT1a domain to PI3P occurs only in the presence of Ca^{2+} ions. Thus, subcellular localization of Atg2 proteins in the ER-phagophore MCSs, a process that is essential for autophagy, may be regulated by Ca^{2+} ions. This is an interesting result, indicating that one of the early steps in the autophagy process is regulated by Ca^{2+} signalling.

To summarize we created the model shown in Fig. 6, which depicts the regulation of the binding of different APT1 domains to membranes. The binding of Vps13 to membranes containing PI3P, such as endosomal membranes, could be achieved in two ways: by interaction of yAPT1v with PI3P and by complementary binding to adaptor proteins such as Ypt35 (Fig. 6B). In the case of chorein, the interacting adaptor protein is not known and the recruitment to PI3P-rich compartments is regulated by ions in the cytoplasm. Because the cellular Mg^{2+} concentration does not change significantly over time, the regulatory effect of Mg^{2+} in cells is weak [64], and rather Ca^{2+} ions control the binding of chorein to PI3P. There are three possible ways for Ca^{2+} to do this. First, Ca^{2+} can interact with the hAPT1 domain and facilitate electrostatic binding to PI3P. Second, the hAPT1 domain can recognize and bind to PI3P, but this binding is not stable, and Ca^{2+} ions can enhance and stabilize this interaction (Fig. 6C). Third, the electrostatic correlation between Ca^{2+} (and any bivalent ions) and the phosphomonoester group of PI3P can be responsible for the enhanced deprotonation of phosphate and, consequently, increasing negative charge leading to strengthening of the interaction between the phospholipids and their effector (Fig. 6D) [65].

Analysis of the impact of the I2771R substitution on the binding to different PIs is important for understanding not only the regulation of interactions between chorein and lipids but for understanding the mechanism of ChAc pathogenesis. The hAPT1 domain modelled by the IonCom server suggests that the I2771R substitution of the chorein is located in the vicinity of amino acid residues that interact with Ca^{2+}. Even though the positive charge provided by arginine could block the binding of Ca^{2+} to the hAPT1 domain this hypothesis was not confirmed when hAPT1* was modelled by IonCom server. Another explanation is that the I2771R substitution triggers structural changes

within the hAPT1 domain, which reduces the interactions with PI3P and PI5P without impacting Ca^{2+} binding but enhances the affinity for PI (Fig. 6E). This enhanced binding of hAPT1* to PI can have a very deleterious effect on cells and can be a reason for the pathogenicity of the mutation. PI3P or PI5P are low-abundance lipids localized to specific membranes, while PI is ubiquitous [66]. Therefore, the ability to interact with PI may result in the loss of specific chorein localization and/or regulation, resulting in a phenotype similar to that caused by the absence of chorein. Interactions with lipids have regulatory consequences for many proteins, and there are many examples of diseases that result from changes in phospholipid metabolism [67]. The mutation I2771R in the APT1 domain of chorein is another example of such a connection.

Here, the biochemical properties of APT1 domains were characterized, and differences between the domains were identified. The obtained results are a basis for further structural studies that should answer questions regarding the structural determinants underlying the differences between APT1 domains, identify amino acid residues that are important for Ca^{2+} ion binding and help to better understand pathogenesis of all *VPS13* and *ATG2*-related diseases.

Supplementary data to this article can be found online at https://doi.org/10.1016/j.bbamem.2020.183349.

Declaration of competing interest

The authors declare that they have no known competing financial interests or personal relationships that could have appeared to influence the work reported in this paper.

Acknowledgements

We would like to acknowledge K. Flis for plasmids and technical support, W. Rzepnikowska for strains and plasmids and A. Kochanski for critical reading of the manuscript. This work was financed by the National Science Centre, Poland. Grant number: UMO-2015/19/B/NZ3/01515 (2016-2020) to T.Z.

References

[1] L. Rampoldi, C. Dobson-Stone, J.P. Rubio, A. Danek, R.M. Chalmers, N.W. Wood, C. Verellen, X. Ferrer, A. Malandrini, G.M. Fabrizi, R. Brown, J. Vance, M. Pericak-Vance, G. Rudolf, S. Carrè, E. Alonso, M. Manfredi, A.H. Németh, A.P. Monaco, A conserved sorting-associated protein is mutant in chorea-acanthocytosis, Nat. Genet. 28 (2) (2001) 119–120.

[2] A. Velayos-Baeza, A. Vettori, R.R. Copley, C. Dobson-Stone, A.P. Monaco, Analysis of the human *VPS13* gene family, Genomics 84 (3) (2004) 536–549.

[3] C. Dobson-Stone, A. Velayos-Baeza, L.A. Filippone, S. Westbury, A. Storch, T. Erdmann, S.J. Wroe, K.L. Leenders, A.E. Lang, M.T. Dotti, A. Federico, S.A. Mohiddin, L. Fananapazir, G. Daniels, A. Danek, A.P. Monaco, Chorein detection for the diagnosis of chorea-acanthocytosis, Ann. Neurol. 56 (2) (2004) 299–302.

[4] S. Ueno, Y. Maruki, M. Nakamura, Y. Tomemori, K. Kamae, H. Tanabe, Y. Yamashita, S. Matsuda, S. Kaneko, A. Sano, The gene encoding a newly discovered protein, chorein, is mutated in chorea-acanthocytosis, Nat. Genet. 28 (2) (2001) 121–122.

[5] H.H. Jung, A. Danek, R.H. Walker, Neuroacanthocytosis syndromes, Orphanet J Rare Dis 6 (2011) 68.

[6] L. De Franceschi, C. Tomelleri, A. Matte, A.M. Brunati, P.H. Bovee-Geurts, M. Bertoldi, E. Lasonder, E. Tibaldi, A. Danek, R.H. Walker, H.H. Jung, B. Bader, A. Siciliano, E. Ferru, N. Mohandas, G.J. Bosman, Erythrocyte membrane changes of chorea-acanthocytosis are the result of altered Lyn kinase activity, Blood 118 (20) (2011) 5652–5663.

[7] I. Alesutan, J. Seifert, T. Pakladok, J. Rheinlaender, A. Lebedeva, S.T. Towhid, C. Stournaras, J. Voelkl, T.E. Schäffer, F. Lang, Chorein sensitivity of actin polymerization, cell shape and mechanical stiffness of vascular endothelial cells, Cell. Physiol. Biochem. 32 (3) (2013) 728–742.

[8] S. Honisch, S. Gu, J.M. Vom Hagen, S. Alkahtani, A.A. Al Kahtane, A. Tsapara, A. Hermann, A. Storch, L. Schöls, F. Lang, C. Stournaras, Chorein sensitive arrangement of cytoskeletal architecture, Cell. Physiol. Biochem. 37 (1) (2015) 399–408.

[9] L. Pelzl, S. Hauser, B. Elsir, B. Sukkar, I. Sahu, Y. Singh, P. Höflinger, R. Bissinger, M. Jemaà, C. Stournaras, L. Schöls, F. Lang, Lithium sensitive ORAI1 expression, store operated Ca, Sci. Rep. 7 (1) (2017) 6457.

[10] N. Stanslowsky, P. Reinhardt, H. Glass, N. Kalmbach, M. Naujock, N. Hensel, V. Lübben, A. Pal, A. Venneri, F. Lupo, L. De Franceschi, P. Claus, J. Sterneckert, A. Storch, A. Hermann, F. Wegner, Neuronal dysfunction in iPSC-derived medium spiny neurons from chorea-acanthocytosis patients is reversed by Src kinase inhibition and F-actin stabilization, J. Neurosci. 36 (47) (2016) 12027–12043.

[11] S. Honisch, B. Fehrenbacher, A. Lebedeva, I. Alesutan, T. Castor, S. Alkahtani, S. Alarifi, M. Schaller, C. Stournaras, F. Lang, Chorein sensitive dopamine release from pheochromocytoma (PC12) cells, Neurosignals 23 (1) (2015) 1–10.

[12] F. Lupo, E. Tibaldi, A. Matte, A.K. Sharma, A.M. Brunati, S.L. Alper, C. Zancanaro, D. Benati, A. Siciliano, M. Bertoldi, F. Zonta, A. Storch, R.H. Walker, A. Danek, B. Bader, A. Hermann, L. De Franceschi, A new molecular link between defective autophagy and erythroid abnormalities in chorea-acanthocytosis, Blood 128 (25) (2016) 2976–2987.

[13] M. Föller, A. Hermann, S. Gu, I. Alesutan, S.M. Qadri, O. Borst, E.M. Schmidt, F. Schiele, J.M. vom Hagen, C. Saft, L. Schöls, H. Lerche, C. Stournaras, A. Storch, F. Lang, Chorein-sensitive polymerization of cortical actin and suicidal cell death in chorea-acanthocytosis, FASEB J. 26 (4) (2012) 1526–1534.

[14] S. Honisch, W. Yu, G. Liu, I. Alesutan, S.T. Towhid, A. Tsapara, S. Schleicher, R. Handgretinger, C. Stournaras, F. Lang, Chorein addiction in *VPS13A* overexpressing rhabdomyosarcoma cells, Oncotarget 6 (12) (2015) 10309–10319.

[15] A. González Montoro, C. Ungermann, StARTing to understand membrane contact sites, Trends Cell Biol. 25 (9) (2015) 497–498.

[16] C.J. Stefan, A.G. Manford, S.D. Emr, ER-PM connections: sites of information transfer and inter-organelle communication, Curr. Opin. Cell Biol. 25 (4) (2013) 434–442.

[17] C. Hönscher, M. Mari, K. Auffarth, M. Bohnert, J. Griffith, W. Geerts, M. van der Laan, M. Cabrera, F. Reggiori, C. Ungermann, Cellular metabolism regulates contact sites between vacuoles and mitochondria, Dev. Cell 30 (1) (2014) 86–94.

[18] A.B. Lang, A.T. John Peter, P. Walter, B. Kornmann, ER-mitochondrial junctions can be bypassed by dominant mutations in the endosomal protein Vps13, J. Cell Biol. 210 (6) (2015) 883–890.

[19] J.S. Park, M.K. Thorsness, R. Policastro, L.L. McGoldrick, N.M. Hollingsworth, P.E. Thorsness, A.M. Neiman, Yeast Vps13 promotes mitochondrial function and is localized at membrane contact sites, Mol. Biol. Cell 27 (15) (2016) 2435–2449.

[20] A.T. John Peter, B. Herrmann, D. Antunes, D. Rapaport, K.S. Dimmer, B. Kornmann, Vps13-Mcp1 interact at vacuole-mitochondria interfaces and bypass ER-mitochondria contact sites, J. Cell Biol. 216 (10) (2017) 3219–3229.

[21] N. Kumar, M. Leonzino, W. Hancock-Cerutti, F.A. Horenkamp, P. Li, J.A. Lees, H. Wheeler, K.M. Reinisch, P. De Camilli, VPS13A and VPS13C are lipid transport proteins differentially localized at ER contact sites, J. Cell Biol. 217 (10) (2018) 3625–3639.

[22] W.M. Yeshaw, M. van der Zwaag, F. Pinto, L.L. Lahaye, A.I. Faber, R. Gómez-Sánchez, A.M. Dolga, C. Poland, A.P. Monaco, S.C. van IJzendoorn, N.A. Grzeschik, A. Velayos-Baeza, O.C. Sibon, Human VPS13A is associated with multiple organelles and influences mitochondrial morphology and lipid droplet motility, Elife 8 (2019).

[23] S.K. Dziurdzik, B.D.M. Bean, M. Davey, E. Conibear, A *VPS13D* spastic ataxia mutation disrupts the conserved adaptor-binding site in yeast Vps13, Hum. Mol. Genet. 29 (4) (2020) 635–648.

[24] W. Rzepnikowska, K. Flis, J. Kaminska, M. Grynberg, A. Urbanek, K.R. Ayscough, T. Zoladek, Amino acid substitution equivalent to human chorea-acanthocytosis I2771R in yeast Vps13 protein affects its binding to phosphatidylinositol 3-phosphate, Hum. Mol. Genet. 26 (8) (2017) 1497–1510.

[25] W. Rzepnikowska, K. Flis, S. Muñoz-Braceras, R. Menezes, R. Escalante, T. Zoladek, Yeast and other lower eukaryotic organisms for studies of Vps13 proteins in health and disease, Traffic 18 (11) (2017) 711–719.

[26] M. De, A.N. Oleskie, M. Ayyash, S. Dutta, L. Mancour, M.E. Abazeed, E.J. Brace, G. Skiniotis, R.S. Fuller, The Vps13p-Cdc31p complex is directly required for TGN late endosome transport and TGN homotypic fusion, J. Cell Biol. 216 (2) (2017) 425–439.

[27] B.D.M. Bean, S.K. Dziurdzik, K.L. Kolehmainen, C.M.S. Fowler, W.K. Kwong, L.I. Grad, M. Davey, C. Schluter, E. Conibear, Competitive organelle-specific adaptors recruit Vps13 to membrane contact sites, J. Cell Biol. 217 (10) (2018) 3593–3607.

[28] D.E. Clapham, Calcium signaling, Cell 131 (6) (2007) 1047–1058.

[29] G. van den Bogaart, K. Meyenberg, U. Diederichsen, R. Jahn, Phosphatidylinositol 4,5-bisphosphate increases Ca^{2+} affinity of synaptotagmin-1 by 40-fold, J. Biol. Chem. 287 (20) (2012) 16447–16453.

[30] M. Mosior, R.M. Epand, Characterization of the calcium-binding site that regulates association of protein kinase C with phospholipid bilayers, J. Biol. Chem. 269 (19) (1994) 13798–13805.

[31] R.S. Aiyar, M. Bohnert, S. Duvezin-Caubet, C. Voisset, J. Gagneur, E.S. Fritsch, E. Couplan, K. von der Malsburg, C. Funaya, F. Soubigou, F. Courtin, S. Suresh, R. Kucharczyk, J. Evrard, C. Antony, R.P. St Onge, M. Blondel, J.P. di Rago, M. van der Laan, L.M. Steinmetz, Mitochondrial protein sorting as a therapeutic target for ATP synthase disorders, Nat. Commun. 5 (2014) 5585.

[32] M. Fukuda, T. Kojima, K. Mikoshiba, Regulation by bivalent cations of phospholipid binding to the C2A domain of synaptotagmin III, Biochem. J. 323 (Pt 2) (1997) 421–5.

[33] J. Kaminska, W. Rzepnikowska, A. Polak, K. Flis, P. Soczewka, K. Bala, M. Sienko, M. Grynberg, P. Kaliszewski, A. Urbanek, K. Ayscough, T. Zoladek, Phosphatidylinositol-3-phosphate regulates response of cells to proteotoxic stress, Int. J. Biochem. Cell Biol. 79 (2016) 494–504.

[34] D.P. Valverde, S. Yu, V. Boggavarapu, N. Kumar, J.A. Lees, T. Walz, K.M. Reinisch, T.J. Melia, ATG2 transports lipids to promote autophagosome biogenesis, J. Cell Biol. 218 (6) (2019) 1787–1798.

[35] A.P. Jacobus, J. Gross, Optimal cloning of PCR fragments by homologous recombination in *Escherichia coli*, PLoS One 10 (3) (2015) e0119221.
[36] L. Zimmermann, A. Stephens, S.Z. Nam, D. Rau, J. Kübler, M. Lozajic, F. Gabler, J. Söding, A.N. Lupas, V. Alva, A completely reimplemented MPI bioinformatics toolkit with a new HHpred server at its Core, J. Mol. Biol. 430 (15) (2018) 2237–2243.
[37] M.N. Wass, L.A. Kelley, M.J. Sternberg, 3DLigandSite: predicting ligand-binding sites using similar structures, Nucleic Acids Res. 38 (2010) W469–W473 Web Server issue).
[38] P. Soczewka, D. Kolakowski, I. Smaczynska-de Rooij, W. Rzepnikowska, K.R. Ayscough, J. Kaminska, T. Zoladek, Yeast-model-based study identified myosin- and calcium-dependent calmodulin signalling as a potential target for drug intervention in chorea-acanthocytosis, Dis. Model. Mech. 12 (1) (2019).
[39] S. Koike, R. Jahn, SNAREs define targeting specificity of trafficking vesicles by combinatorial interaction with tethering factors, Nat. Commun. 10 (1) (2019) 1608.
[40] J.O. De Craene, D.L. Bertazzi, S. Bär, S. Friant, Phosphoinositides, major actors in membrane trafficking and lipid signaling pathways, Int. J. Mol. Sci. 18 (3) (2017).
[41] J.H. Brickner, R.S. Fuller, *SOI1* encodes a novel, conserved protein that promotes TGN-endosomal cycling of Kex2p and other membrane proteins by modulating the function of two TGN localization signals, J. Cell Biol. 139 (1) (1997) 23–36.
[42] S. Muñoz-Braceras, R. Calvo, R. Escalante, TipC and the chorea-acanthocytosis protein VPS13A regulate autophagy in *Dictyostelium* and human HeLa cells, Autophagy 11 (6) (2015) 918–927.
[43] J. Hasegawa, B.S. Strunk, L.S. Weisman, PI5P and PI(3,5)P, Cell Struct. Funct. 42 (1) (2017) 49–60.
[44] D. Sarkes, L.E. Rameh, A novel HPLC-based approach makes possible the spatial characterization of cellular PtdIns5P and other phosphoinositides, Biochem. J. 428 (3) (2010) 375–384.
[45] J. Viaud, F. Lagarrigue, D. Ramel, S. Allart, G. Chicanne, L. Ceccato, D. Courilleau, J.M. Xuereb, O. Pertz, B. Payrastre, F. Gaits-Iacovoni, Phosphatidylinositol 5-phosphate regulates invasion through binding and activation of Tiam1, Nat. Commun. 5 (2014) 4080.
[46] K. Niebuhr, S. Giuriato, T. Pedron, D.J. Philpott, F. Gaits, J. Sable, M.P. Sheetz, C. Parsot, P.J. Sansonetti, B. Payrastre, Conversion of PtdIns(4,5)P(2) into PtdIns(5)P by the *S.flexneri* effector IpgD reorganizes host cell morphology, EMBO J. 21 (19) (2002) 5069–5078.
[47] C. Pendaries, H. Tronchère, L. Arbibe, J. Mounier, O. Gozani, L. Cantley, M.J. Fry, F. Gaits-Iacovoni, P.J. Sansonetti, B. Payrastre, PtdIns5P activates the host cell PI3-kinase/Akt pathway during *Shigella flexneri* infection, EMBO J. 25 (5) (2006) 1024–1034.
[48] J.H. Clarke, A.J. Letcher, C.S. D'santos, J.R. Halstead, R.F. Irvine, N. Divecha, Inositol lipids are regulated during cell cycle progression in the nuclei of murine erythroleukaemia cells, Biochem. J. 357(Pt 3) (2001) 905–10.
[49] O. Gozani, P. Karuman, D.R. Jones, D. Ivanov, J. Cha, A.A. Lugovskoy, C.L. Baird, H. Zhu, S.J. Field, S.L. Lessnick, J. Villasenor, B. Mehrotra, J. Chen, V.R. Rao, J.S. Brugge, C.G. Ferguson, B. Payrastre, D.G. Myszka, L.C. Cantley, G. Wagner, N. Divecha, G.D. Prestwich, J. Yuan, The PHD finger of the chromatin-associated protein ING2 functions as a nuclear phosphoinositide receptor, Cell 114 (1) (2003) 99–111.
[50] D.R. Jones, Y. Bultsma, W.J. Keune, J.R. Halstead, D. Elouarrat, S. Mohammed, A.J. Heck, C.S. D'Santos, N. Divecha, Nuclear PtdIns5P as a transducer of stress signaling: an in vivo role for PIP4Kbeta, Mol. Cell 23 (5) (2006) 685–695.
[51] F. Boal, R. Mansour, M. Gayral, E. Saland, G. Chicanne, J.M. Xuereb, M. Marcellin, O. Burlet-Schiltz, P.J. Sansonetti, B. Payrastre, H. Tronchère, TOM1 is a PI5P effector involved in the regulation of endosomal maturation, J. Cell Sci. 128 (4) (2015) 815–827.
[52] A. Shisheva, D. Sbrissa, O. Ikonomov, Plentiful PtdIns5P from scanty PtdIns(3,5)P2 or from ample PtdIns? PIKfyve-dependent models: evidence and speculation (response to: DOI 10.1002/bies.201300012), Bioessays 37 (3) (2015) 267–277.
[53] A. Shisheva, PtdIns5P: news and views of its appearance, disappearance and deeds, Arch. Biochem. Biophys. 538 (2) (2013) 171–180.
[54] R.V. Stahelin, J.L. Scott, C.T. Frick, Cellular and molecular interactions of phosphoinositides and peripheral proteins, Chem. Phys. Lipids 182 (2014) 3–18.
[55] W.K. Huh, J.V. Falvo, L.C. Gerke, A.S. Carroll, R.W. Howson, J.S. Weissman, E.K. O'Shea, Global analysis of protein localization in budding yeast, Nature 425 (6959) (2003) 686–691.
[56] M.A. Lemmon, Pleckstrin homology (PH) domains and phosphoinositides, Biochem. Soc. Symp. 74 (2007) 81–93.
[57] R. Babazadeh, D. Ahmadpour, S. Jia, X. Hao, P. Widlund, K. Schneider, F. Eisele, L.D. Edo, G.J. Smits, B. Liu, T. Nystrom, Syntaxin 5 is required for the formation and clearance of protein inclusions during proteostatic stress, Cell Rep. 28 (8) (2019) 2096–2110.e8.
[58] R. Gómez-Sánchez, J. Rose, R. Guimarães, M. Mari, D. Papinski, E. Rieter, W.J. Geerts, R. Hardenberg, C. Kraft, C. Ungermann, F. Reggiori, Atg9 establishes Atg2-dependent contact sites between the endoplasmic reticulum and phagophores, J. Cell Biol. 217 (8) (2018) 2743–2763.
[59] W. Cho, R.V. Stahelin, Membrane binding and subcellular targeting of C2 domains, Biochim. Biophys. Acta 1761 (8) (2006) 838–849.
[60] K. Suzuki, M. Akioka, C. Kondo-Kakuta, H. Yamamoto, Y. Ohsumi, Fine mapping of autophagy-related proteins during autophagosome formation in *Saccharomyces cerevisiae*, J. Cell Sci. 126(Pt 11) (2013) 2534–44.
[61] D. Romanyuk, A. Polak, A. Maleszewska, M. Sienko, M. Grynberg, T. Zoladek, Human hAtg2A protein expressed in yeast is recruited to preautophagosomal structure but does not complement autophagy defects of *atg2Δ* strain, Acta Biochim. Pol. 58 (3) (2011) 365–374.
[62] S.G. Pfisterer, M. Mauthe, P. Codogno, T. Proikas-Cezanne, Ca2+/calmodulin-dependent kinase (CaMK) signaling via CaMKI and AMP-activated protein kinase contributes to the regulation of WIPI-1 at the onset of autophagy, Mol. Pharmacol. 80 (6) (2011) 1066–1075.
[63] A. Grotemeier, S. Alers, S.G. Pfisterer, F. Paasch, M. Daubrawa, A. Dieterle, B. Viollet, S. Wesselborg, T. Proikas-Cezanne, B. Stork, AMPK-independent induction of autophagy by cytosolic Ca^{2+} increase, Cell. Signal. 22 (6) (2010) 914–925.
[64] A.M. Romani, Cellular magnesium homeostasis, Arch. Biochem. Biophys. 512 (1) (2011) 1–23.
[65] W. Wang, N.A. Anderson, A. Travesset, D. Vaknin, Regulation of the electric charge in phosphatidic acid domains, J. Phys. Chem. B 116 (24) (2012) 7213–7220.
[66] E.J. Dickson, B. Hille, Understanding phosphoinositides: rare, dynamic, and essential membrane phospholipids, Biochem. J. 476 (1) (2019) 1–23.
[67] H.J. McCrea, P. De Camilli, Mutations in phosphoinositide metabolizing enzymes and human disease, Physiology (Bethesda) 24 (2009) 8–16.